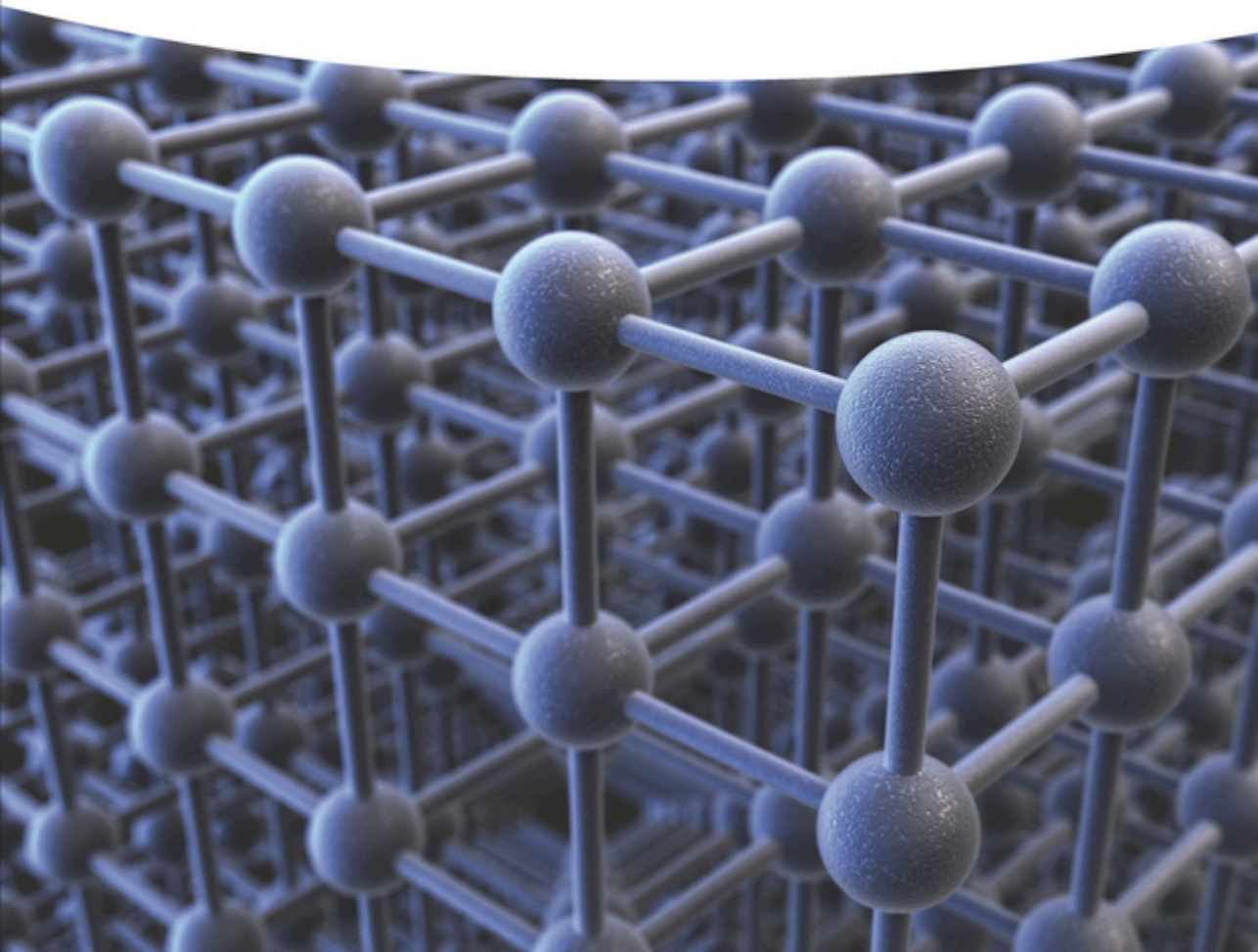


Emil Zolotoyabko

Introduction to Solid State Physics for Materials Engineers



Introduction to Solid State Physics for Materials Engineers

Introduction to Solid State Physics for Materials Engineers

Emil Zolotoyabko

WILEY-VCH

Author

Professor Emil Zolotoyabko

Technion - Israel Institute of Technology
Department of Materials Science and
Engineering
Technion City
32000 Haifa
Israel

■ All books published by **WILEY-VCH** are carefully produced. Nevertheless, authors, editors, and publisher do not warrant the information contained in these books, including this book, to be free of errors. Readers are advised to keep in mind that statements, data, illustrations, procedural details or other items may inadvertently be inaccurate.

Library of Congress Card No.:
applied for

British Library Cataloguing-in-Publication Data

A catalogue record for this book is available from the British Library.

Bibliographic information published by the Deutsche Nationalbibliothek

The Deutsche Nationalbibliothek lists this publication in the Deutsche Nationalbibliografie; detailed bibliographic data are available on the Internet at <<http://dnb.d-nb.de>>.

© 2021 WILEY-VCH GmbH, Boschstr. 12, 69469 Weinheim, Germany

All rights reserved (including those of translation into other languages). No part of this book may be reproduced in any form – by photoprinting, microfilm, or any other means – nor transmitted or translated into a machine language without written permission from the publishers. Registered names, trademarks, etc. used in this book, even when not specifically marked as such, are not to be considered unprotected by law.

Print ISBN: 978-3-527-34884-8

ePDF ISBN: 978-3-527-83158-6

ePub ISBN: 978-3-527-83159-3

Typesetting SPi Global, Chennai, India

Printed on acid-free paper

10 9 8 7 6 5 4 3 2 1

*To My Wife Roza With the Deepest Feeling of Gratitude for Her Life-Long Love,
Support, and Assistance*

Contents

Preface *xi*

Introduction *xiii*

- 1 General Impact of Translational Symmetry in Crystals on Solid State Physics** *1*
 - 1.1 Crystal Symmetry in Real Space *3*
 - 1.2 Symmetry and Physical Properties in Crystals *9*
 - 1.3 Wave Propagation in Periodic Media and Construction of Reciprocal Lattice *13*
 - 1.A Symmetry Constraints on Rotation Axes *18*
 - 1.B Twinning in Crystals *20*

- 2 Electron Waves in Crystals** *23*
 - 2.1 Electron Behavior in a Periodic Potential and Energy Gap Formation *23*
 - 2.2 The Brillouin Zone *28*
 - 2.3 Band Structure *31*
 - 2.4 Graphene *35*
 - 2.5 Fermi Surface *40*
 - 2.A Cyclotron Resonance and Related Phenomena *43*

- 3 Elastic Wave Propagation in Periodic Media, Phonons, and Thermal Properties of Crystals** *51*
 - 3.1 Linear Chain of the Periodically Positioned Atoms *51*
 - 3.2 Phonons and Heat Capacity *56*
 - 3.3 Thermal Vibrations of Atoms in Crystals *59*
 - 3.4 Crystal Melting *60*
 - 3.5 X-ray and Neutron Interaction with Phonons *61*
 - 3.5.1 Debye–Waller Factor *65*
 - 3.6 Lattice Anharmonicity *67*
 - 3.7 Velocities of Bulk Acoustic Waves *69*
 - 3.8 Surface Acoustic Waves *72*
 - 3.A Bose’s Derivation of the Planck Distribution Function *73*

4	Electrical Conductivity in Metals	75
4.1	Classical Drude Theory	76
4.2	Quantum–Mechanical Approach	77
4.3	Phonon Contribution to Electrical Resistivity	80
4.4	Defects’ Contributions to Metal Resistivity	82
4.A	Derivation of the Fermi-Dirac Distribution Function	84
5	Electron Contribution to Thermal Properties of Crystals	87
5.1	Electronic Specific Heat	87
5.2	Electronic Heat Conductivity and the Wiedemann–Franz Law	92
5.3	Thermoelectric Phenomena	94
5.4	Thermoelectric Materials	98
6	Electrical Conductivity in Semiconductors	105
6.1	Intrinsic (Undoped) Semiconductors	105
6.2	Extrinsic (Doped) Semiconductors	110
6.3	<i>p</i> – <i>n</i> Junction	111
6.4	Semiconductor Transistors	117
6.A	Estimation of Exciton’s Radius and Binding Energy	120
7	Work Function and Related Phenomena	123
7.1	Work Function of Metals	123
7.2	Photoelectric Effect	126
7.2.1	Angle-Resolved Photoemission Spectroscopy (APRES)	126
7.3	Thermionic Emission	128
7.4	Metal-Semiconductor Junction	131
7.A	Image Charge Method	133
7.B	A Free Electron Cannot Absorb a Photon	134
8	Light Interaction with Metals and Dielectrics	135
8.1	Skin Effect in Metals	137
8.2	Light Reflection from a Metal	138
8.3	Plasma Frequency	140
8.4	Introduction to Metamaterials	141
8.5	Structural Colors	148
8.A	Acoustic Metamaterials	150
9	Light Interaction with Semiconductors	155
9.1	Solar Cells	155
9.1.1	The Grätzel Cell	159
9.1.2	Halide Perovskite Solar Cells	161
9.2	Solid State Radiation Detectors	162
9.2.1	Infrared Detectors	164
9.3	Charge-Coupled Devices (CCDs)	167
9.4	Light-Emitting Diodes (LEDs)	168

9.5	Semiconductor Lasers	170
9.6	Photonic Materials	173
10	Cooperative Phenomena in Electron Systems: Superconductivity	177
10.1	Phonon-Mediated Cooper Pairing Mechanism	178
10.2	Direct Measurements of the Superconductor Energy Gap	182
10.3	Josephson Effect	184
10.4	Meissner Effect	185
10.5	SQUID	188
10.6	High-Temperature Superconductivity	189
10.A	Fourier Transform of the Coulomb Potential	192
10.B	The Josephson Effect Theory	193
10.C	Derivation of the Critical Magnetic Field in Type I Superconductors	195
11	Cooperative Phenomena in Electron Systems: Ferromagnetism	197
11.1	Paramagnetism and Ferromagnetism	198
11.2	The Ising Model	204
11.3	Magnetic Structures	205
11.4	Magnetic Domains	207
11.5	Magnetic Materials	210
11.6	Giant Magnetoresistance	211
11.A	The Elementary Magnetic Moment of an Electron Produced by its Orbital Movement	214
11.B	Pauli Paramagnetism	214
11.C	Magnetic Domain Walls	216
12	Ferroelectricity as a Cooperative Phenomenon	219
12.1	The Theory of Ferroelectric Phase Transition	223
12.2	Ferroelectric Domains	227
12.3	The Piezoelectric Effect and Its Application in Ferroelectric Devices	230
12.4	Other Application Fields of Ferroelectrics	233
13	Other Examples of Cooperative Phenomena in Electron Systems	237
13.1	The Mott Metal–Insulator Transition	237
13.2	Classical and Quantum Hall Effects	241
13.3	Topological Insulators	247
13.A	Electron Energies and Orbit Radii in the Simplified Bohr Model of a Hydrogen-like Atom	250
	Further Reading	253
	List of Prominent Scientists Mentioned in the Book	255
	Index	265

Preface

Powerful personal computers and smart phones, huge flat TV screens and bright shining lights in our streets and city squares, immense fields of solar cells providing clean electrical energy, infrared imaging and laser technologies, strong superconducting magnets used in particle accelerators and medical devices for magnetic resonance imaging (MRI) – all these and many other things surrounding us are the outcome of discoveries and inventions made during the development of solid state physics. It is a rather young branch of science which began to advance only at the beginning of twentieth century. Though, as we see, its impact on society is tremendous and continues to grow with time. For this reason, learning solid state physics is obligatory for materials scientists and engineers.

There exist many excellent solid-state physics textbooks. Some of these, however, especially general books written by theoreticians for physicists, are difficult for materials engineers to use because of the latter's insufficient knowledge in advanced quantum mechanics. Further, these books pay much less attention to key applications (new materials and devices). In contrast, more specialized manuscripts written by experts in specific fields do not provide a big picture since they mostly deal with practically important issues with less emphasis on basic ideas.

Very few books have tried to fill this gap. One of the best, in my opinion, is "Intermediate quantum theory of crystalline solids" by Alexander Animalu from MIT. It was published, however, in 1977, and since then many new branches of solid state physics have been developed, such as high-temperature superconductivity, giant magnetoresistance, photovoltaics, graphene, Mott metal-insulator transitions, quantum Hall effects, topological insulators, etc. All these, as well as traditional classical issues, are described in the present book together with the most important applications such as MOSFET transistors, permanent and superconducting magnets, thermoelectric materials, solar cells and light-emitting diodes, metamaterials, photonic materials, magnetic and ferroelectric memories, SQUID, infrared detectors, and CCD.

To be able to read this book, it is enough to have very basic knowledge of mechanics, thermodynamics, electricity and magnetism, quantum mechanics, plus a little familiarity with statistical physics. More complicated issues or those that could be omitted during a first reading will be found in the Appendices.

Mathematical tools are restricted by simple differential equations, vector algebra and a bit of tensors (matrices), which all are familiar to materials students.

The book comprises 13 chapters, which are used as the basis for 13 lectures of the one-semester solid-state physics course delivered in the Department of Materials Science and Engineering at the Technion-Israel Institute of Technology. Before each chapter, the list of sub-subjects touched upon in it is given, which is wider than the list of numerated subsections. Certainly, not all aspects of solid-state physics are covered. For example, amorphous and highly disordered systems are not within this book's scope. This book is intended for the wide community of undergraduate and graduate students in materials science and engineering, as well as for beginners who for some reasons are interested in particular aspects of solid state physics. In summary, this book can be considered as an extended introduction to the subject, which will enable its readers to be well prepared for understanding of more advanced textbooks, if needed.

Haifa
March 2021

Introduction

If we consider a crystalline state, the quintessence of solid state physics is the propagation of electron waves and acoustic waves (phonons) in a medium with translational symmetry and further interaction of electrons with phonons and photons, as well as an interaction between electrons themselves. This statement determines the structure of the present book.

The book starts with a discussion of the general impact of translational symmetry in crystals on solid state physics (Chapter 1) and includes a brief description of crystal symmetry in real space; the interrelation between symmetry and physical properties in crystals; wave propagation in periodic media and construction of reciprocal lattices; and qualitative considerations regarding the diffraction of valence electrons on periodic lattice potential and band gap formation.

In Chapter 2, the band gap formation at the Brillouin zone boundary is quantitatively treated by solving the Schrödinger equation in periodic medium. In addition, the structure of energy bands in metals, semiconductors, and insulators is considered, including some aspects of orbital hybridization and the band structure of graphene. At the end of this chapter we discuss the concept of a Fermi surface, its measurement by different methods and its connection to electron conduction.

Chapter 3 is devoted to elastic wave propagation in crystals and includes definitions of acoustic and optical phonons, and a description of the thermal properties of crystals. Here we introduce Debye temperature and Bose–Einstein statistics. Additionally, we show how to calculate the velocities of bulk acoustic waves and surface (Rayleigh) acoustic waves.

In Chapter 4, we deal with electrical conductivity in metals in the framework of classical Drude theory and performing quantum–mechanical calculations. Contributions to metal resistivity from electron scattering by phonons and lattice defects are thoroughly analyzed. Here we introduce Fermi–Dirac statistics and establish the interrelation between Fermi energy and chemical potential.

In Chapter 5, we consider the electron contribution to thermal properties of crystals: electronic specific heat and the electronic part of thermal conductivity. We also discuss the interrelation between electrical conductivity and thermal conductivity in metals, which leads to the Wiedemann–Franz law. The rest of the chapter is devoted to thermoelectricity, i.e. the Seebeck, Peltier, and Thomson effects, and thermoelectric materials with a high figure of merit.

Chapter 6 is devoted to electrical conductivity via electrons and holes in intrinsic (undoped) and doped semiconductors. In this chapter the p - n junction concept is introduced and the key phenomenon of band bending in the depletion region is analytically derived. Further, the working principles of semiconductor diodes and transistors are described, including the metal-oxide-semiconductor field-effect transistor (MOSFET).

Chapter 7 is dedicated to contact phenomena arising at the boundary between a metal and a vacuum, as well as at the metal–semiconductor junctions (Schottky contacts). We introduce the important concept of work function and describe methods to measure it by a Kelvin probe, the photoelectric effect or angle-resolved photoemission spectroscopy (APRES). After that, thermionic emission at elevated temperatures and under electric field application is comprehensively treated, bearing in mind the utmost importance of the latter for an invention of field-emission gun.

In Chapters 8 and 9, we discuss light (photon) interaction with materials. In Chapter 8, we describe some key issues regarding this in metals and insulators. Among them are skin effect, light reflection from metal surfaces, plasma frequency, metamaterials, and structural colors. In Chapter 9, we discuss light interaction with semiconductors. Particular topics include photovoltaics, solar cells, solid state radiation detectors, charge-coupled device (CCD), light-emitting diodes, semiconductor lasers, and photonic materials.

The last four chapters are dedicated to cooperative (correlated) phenomena in electron and ion systems. For example, in Chapter 10, we consider superconductivity. The discussed issues include: Cooper pair formation, isotope effect, Giaever tunneling and the Josephson effect, the Meissner effect, superconductors of type I and type II, superconducting magnets, the superconducting quantum interference device (SQUID), and high temperature superconductivity.

Chapter 11 is devoted to ferromagnetism. Sub-subjects comprise determination of atomic magnetic moments, paramagnetism and diamagnetism, the Weiss molecular field, spontaneous magnetization, exchange interaction, the Ising model, magnetic structures, the subdivision of magnetic materials into ferromagnetics, antiferromagnetics and ferrimagnetics, magnetic domains and domain walls, and giant magnetoresistance.

Chapter 12 is called “Ferroelectricity as cooperative phenomenon.” Here we discuss the following issues: ferroelectric crystals, ferroelectric phase transitions in the framework of Landau–Ginzburg theory, dielectric permittivity near the Curie temperature, ferroelectric domains and domain walls, piezoelectric effect in ferroelectrics, and ferroelectrics-based devices.

Other examples of cooperative phenomena in electron systems are given in Chapter 13. They include metal–insulator (Mott) transition and quantum Hall effects: integer and fractional, and topological insulators.

1

General Impact of Translational Symmetry in Crystals on Solid State Physics

Atomic order in crystals.
Local and translational symmetries.
Symmetry impact on physical properties in crystals.
Wave propagation in periodic media.
Quasi-momentum conservation law.
Reciprocal space.
Wave diffraction conditions.
Degeneracy of electron energy states at the Brillouin zone boundary.
Diffraction of valence electrons and bandgap formation.

In contrast to liquids or gases, atoms in a solid state, in average (over time), are located at fixed atomic positions. The thermally assisted movements around them or between them are strongly limited in space (as for thermal vibrations in potential wells) or have rather low probabilities (as for long-range atomic diffusion). According to the types of the averaged long-range atomic arrangements, all solid materials can be sub-divided into the three following classes, i.e. regular crystals, amorphous materials, and quasicrystals.

Most solid materials are regular (conventional) crystals with fully ordered and periodic atomic arrangements, which can be described by the set of translated elementary blocks (unit cells) densely covering the space with no voids. Nowadays, using the advanced characterization methods, such as high-resolution electron microscopy or scanning tunneling microscopy, it is possible to directly visualize this atomic periodicity (Figure 1.1). Due to the translational symmetry, the key phenomenon – namely, diffraction of short-wavelength quantum beams (electrons, X-rays, neutrons) – takes place. As we show in the following text, sharp diffraction peaks (or spots), which are the “visiting card” of crystalline state, are originated from the quasi-momentum (quasi-wavevector) conservation law in 3D.

In contrary, amorphous materials, being characterized by some kind of short-range ordering, do not reveal atomic order on a long range (Figure 1.2). In other words, certain correlations between atomic positions exist within a few first coordination spheres only and rapidly attenuate and disappear at longer distances.

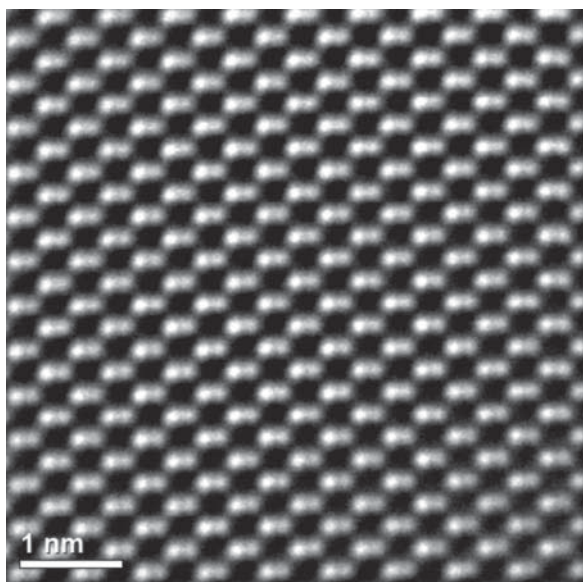


Figure 1.1 High-resolution scanning transmission electron microscopy image of atomic columns in crystalline GaSb. Cations and anions within dumbbells are separated by 0.15 nm.

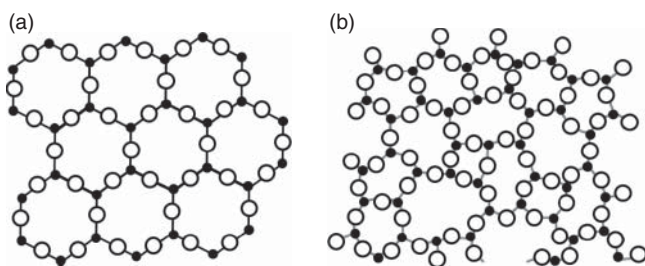


Figure 1.2 Structural motifs in silicon dioxide (SiO_2): (a) – ordered atomic arrangement in crystalline quartz; (b) – disordered arrangement in amorphous silica. Large open circles and black filled circles indicate oxygen and silicon atoms, respectively.

Correspondingly, diffraction patterns taken from amorphs show diffuse features only (called amorphous halo), rather than sharp diffraction peaks.

Quasicrystals in some sense occupy a niche between crystals and amorphs. They have been discovered in the beginning of 1980s by **Dan Shechtman** during his studies (by electron diffraction) of the structure of rapidly solidified Al–Mn alloys. Quasicrystals can be described as fully ordered, *but non-periodic arrangements* of elementary blocks densely covering the space with no voids. An example of filling the 2D space in this fashion, by the so-called **Penrose tiles** (rhombs having smaller angles equal 18° and 72°), is shown in Figure 1.3. Amazingly that despite the lack of the long-range translational symmetry, quasicrystals, like regular crystals, also produce sharp diffraction peaks (or spots), their positions being defined by the quasi-momentum conservation law in high-dimensional space (higher than 3D, see Section 1.1). In this high-dimensional space (hyperspace), quasicrystals are periodic entities, their periodicity being lost when projecting them onto real 3D space.

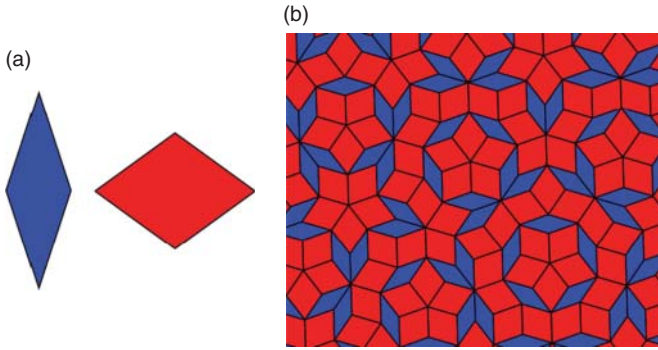


Figure 1.3 Dense filling of 2D space by spatially ordered, though non-periodic **Penrose** tiles (b). Fivefold symmetry regions (regular pentagons) are clearly seen across the pattern. Elemental shapes composing this tiling, i.e. two rhombs with smaller angles equal 18° (blue) and 72° (red), are shown in the (a).

In 1992, based on these findings, the International Union of Crystallography changed the definition of a crystal toward uniting the regular crystals and quasicrystals under single title with an emphasis on the similarity of diffraction phenomena: “A material is a crystal if it has *essentially* a sharp diffraction pattern. The word *essentially* means that most of the intensity of the diffraction is concentrated in relatively sharp **Bragg** peaks, besides the always present diffuse scattering.” In 2011, **Dan Shechtman** was awarded Nobel Prize in Chemistry “for the discovery of quasicrystals.”

1.1 Crystal Symmetry in Real Space

Across this book, we will focus on physical properties of regular crystals, amorphs and quasicrystals being out of our scope here. Thinking on conventional crystals, we first keep in mind their translational symmetry. As we already mentioned, the long-range periodic order in crystals leads to translational symmetry, which is commonly described in terms of **Bravais** lattices (named after French crystallographer **Auguste Bravais**):

$$\mathbf{r}_s = n_1 \mathbf{a}_1 + n_2 \mathbf{a}_2 + n_3 \mathbf{a}_3 \quad (1.1)$$

The nodes, \mathbf{r}_s , of **Bravais** lattice are produced by linear combinations of three non-coplanar vectors, \mathbf{a}_1 , \mathbf{a}_2 , \mathbf{a}_3 , called translation vectors. The integer numbers in Eq. (1.1) can be positive, negative, or zero. Atomic arrangements within every crystal can be described by the set of analogous **Bravais** lattices.

Classification of **Bravais** lattices is based on the relationships between the lengths of translation vectors, $|\mathbf{a}_1| = a$, $|\mathbf{a}_2| = b$, $|\mathbf{a}_3| = c$ and the angles, α , β , γ , between them. In fact, all possible types of **Bravais** lattices can be attributed to seven symmetry systems:

Triclinic: $a \neq b \neq c$ and $\alpha \neq \beta \neq \gamma$;

Monoclinic: $a \neq b \neq c$ and $\alpha = \beta = 90^\circ$, $\gamma \neq 90^\circ$; in this setting, angle γ is between translation vectors \mathbf{a}_1 ($|\mathbf{a}_1| = a$) and \mathbf{a}_2 ($|\mathbf{a}_2| = b$); whereas the angles α and β are, respectively, between translation vectors $\mathbf{a}_2 \wedge \mathbf{a}_3$ and $\mathbf{a}_1 \wedge \mathbf{a}_3$;

Orthorhombic: $a \neq b \neq c$ and $\alpha = \beta = \gamma = 90^\circ$;

Tetragonal: $a = b \neq c$ and $\alpha = \beta = \gamma = 90^\circ$;

Cubic: $a = b = c$ and $\alpha = \beta = \gamma = 90^\circ$;

Rhombohedral: $a = b = c$ and $\alpha = \beta = \gamma \neq 90^\circ$;

Hexagonal: $a = b \neq c$ and $\alpha = \beta = 90^\circ$, $\gamma = 120^\circ$.

A parallelepiped built by the aid of vectors \mathbf{a}_1 , \mathbf{a}_2 , \mathbf{a}_3 is called a unit cell and is the smallest block, which being duplicated by the translation vectors allows us to densely fill the 3D space without voids.

Translational symmetry, however, is only a part of the whole symmetry in crystals. Atomic networks, described by **Bravais** lattices, also possess the so-called local (point) symmetry, which includes lattice inversion with respect to certain lattice points, mirror reflections in some lattice planes, and lattice rotations about certain rotation axes (certain crystallographic directions). After application of all these symmetry elements, the lattice remains invariant. Furthermore, rotation axes are defined by their order, n . The latter, in turn, determines the minimum angle, $\varphi = \frac{360^\circ}{n}$, after rotation by which the lattice remains indistinguishable with respect to its initial setting (lattice invariance). In regular crystals, the permitted rotation axes, i.e. those matching translational symmetry (see Appendix 1.A), are twofold (180° -rotation, $n = 2$), threefold (120° -rotation, $n = 3$), fourfold (90° -rotation, $n = 4$), and sixfold (60° -rotation, $n = 6$). Of course, onefold, i.e. 360° -rotation ($n = 1$), is a trivial symmetry element existing in every **Bravais** lattice. The international notations for these symmetry elements are: $\bar{1}$ - for inversion center, m - for mirror plane, and $1, 2, 3, 4, 6$ - for respective rotation axes. We see that fivefold rotation axis and axes of the order, higher than $n = 6$, are incompatible with translational symmetry (see Appendix 1.A).

To deeper understand why some rotation axes are permitted, while others not, let us consider the covering of the 2D space by regular geometrical figures, having n equal edges and central angle, $\varphi = \frac{360^\circ}{n}$ (Figure 1.4). Correspondingly, the angle, δ , between adjacent edges is:

$$\delta = 180^\circ - \varphi = 180^\circ - \frac{360^\circ}{n} \quad (1.2)$$

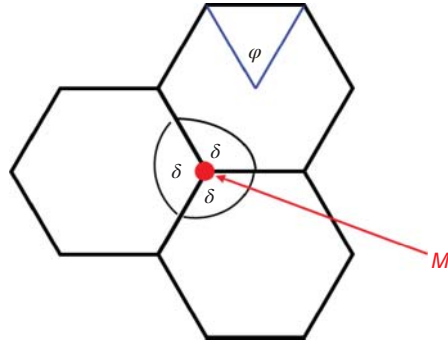
To produce a pattern without voids by using these figures, we require that the full angle around each meeting point, M, defined by p adjacent figures, should be 360° , i.e. $p \cdot \delta = 360^\circ$. Therefore, using Eq. (1.2) yields:

$$p\delta = p \left[180^\circ - \frac{360^\circ}{n} \right] = 360^\circ \quad (1.3)$$

or

$$\frac{1}{2} - \frac{1}{n} = \frac{1}{p} \quad (1.4)$$

Figure 1.4 Dense filling of 2D space by regular geometrical figures.



Finally, we obtain:

$$p = \frac{2n}{n-2} = 2 + \frac{4}{n-2} \quad (1.5)$$

It follows from Eq. (1.5) that there is a very limited set of regular figures (with $2 < n \leq 6$) useful for producing periodic patterns, which fill the 2D space with no voids (i.e. providing integer numbers, p). These are hexagons ($n = 6, p = 3, \varphi = 60^\circ$), squares ($n = 4, p = 4, \varphi = 90^\circ$), and triangles ($n = 3, m = 6, \varphi = 120^\circ$). Based on the value of central angle, φ , these regular figures possess the sixfold, fourfold, and threefold rotation axes, respectively. Since they are related to regular geometrical figures, these rotation axes are called high-symmetry elements. Regarding the twofold axis, it fits the symmetry of the parallelogram, which also can be used for filling the 2D space without voids but does not represent a regular geometrical figure. For this reason, the twofold rotation axis is classified as a low symmetry element (together with inversion center, $\bar{1}$, and mirror plane, m). It also comes out from Eq. (1.5), that regular figures with fivefold rotation axis ($n = 5$), as well as with rotation axes higher than $n > 6$, are incompatible with translational symmetry, i.e. cannot be used for producing periodic patterns without voids since parameter, p , is not an integer number.

In the absence of the long-range translational symmetry, however, as in quasicrystals, one can find additional rotation axes, e.g. fivefold ($\varphi = \frac{360^\circ}{5} = 72^\circ$), as for 2D construction shown in Figure 1.3 or for icosahedral symmetry in 3D. The latter can be found in two **Platonic** bodies: regular icosahedrons and dodecahedrons. Regular dodecahedron has 12 pentagonal faces and 20 vertices, in each of them three faces meet (Figure 1.5). Therefore, the fivefold axes are normal to the pentagonal faces. In contrast, regular icosahedron has 20 triangular faces and 12 vertices, in each of them five faces meet (Figure 1.6). Therefore, the fivefold axes connect the body center and each vertex. Note that regular pentagon (plane figure) has central angle 72° and is characterized by the so-called golden ratio τ (the ratio between the pentagon diagonal, d_p , and pentagon edge, a_p , see Figure 1.7):

$$\tau = \frac{d_p}{a_p} = 2 \cos 36^\circ = \frac{1 + \sqrt{5}}{2} = 1.681 \quad (1.6)$$

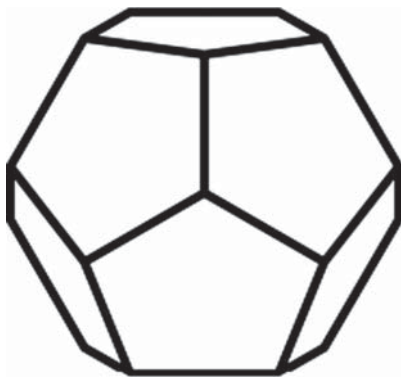


Figure 1.5 Dodecahedron sculpted by 12 pentagonal faces.



Figure 1.6 Icosahedron sculpted by 20 triangular faces.

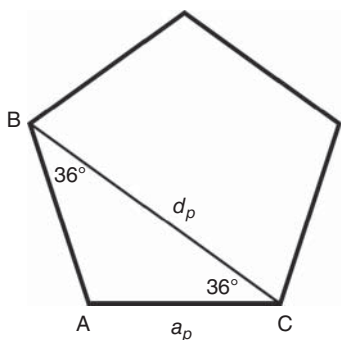


Figure 1.7 Regular pentagon with edges equal a_p and diagonals equal d_p . The ratio, $\frac{BC}{AC} = \frac{d_p}{a_p} = 2 \cos 36^\circ = \frac{1+\sqrt{5}}{2}$, is called the golden ratio (Eq. (1.6)).

which is of great importance to the quasicrystal diffraction conditions (described later in this chapter).

Permitted combinations of local symmetry elements (totally 32 in regular crystals) are called point groups. A set of different crystals, possessing the same point group symmetry, form certain crystal class. Point group symmetry is responsible for

Figure 1.8 Unit cells of the following side-centered **Bravais** lattices: A-type (a), B-type (b), C-type (c). Translation vectors, \mathbf{a}_1 , \mathbf{a}_2 , \mathbf{a}_3 , are indicated by dashed arrows.

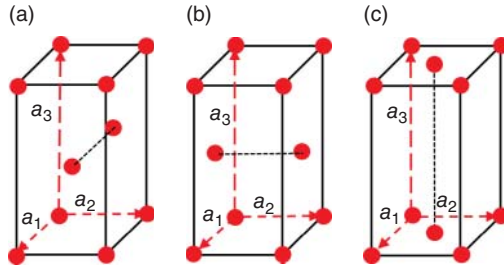
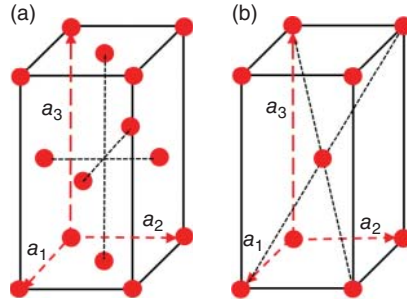


Figure 1.9 Unit cells of the following centered **Bravais** lattices: (a) face-centered (F-type) and (b) body-centered (I-type). Translation vectors, \mathbf{a}_1 , \mathbf{a}_2 , \mathbf{a}_3 , are indicated by dashed arrows.



anisotropy of physical properties in crystals, as explained in more detail further in this chapter.

Bravais lattices defined by Eq. (1.1) are primitive (P) since they effectively contain only one atom per unit cell. However, in some symmetry systems, the same local symmetry will be held for centered **Bravais** lattices, in which the symmetry-related equivalent points are not only the corners (vertices) of the unit cell (as for primitive lattice), but also the centers of the unit cell faces or the geometrical center of the unit cell itself (Figures 1.8 and 1.9). Such lattices are conventionally called *side-centered* (A, B, or C), *face-centered* (F), and *body-centered* (I). In side-centered modifications of the type A, B, or C, additional equivalent points are in the centers of two opposite faces, being perpendicular, respectively, to the \mathbf{a}_1 -, \mathbf{a}_2 -, or \mathbf{a}_3 - translation vectors (Figure 1.8). In the face-centered modification, F, all faces of the **Bravais** parallelepiped (unit cell) are centered (Figure 1.9). For the cubic symmetry system, the F-centered **Bravais** lattice is called face-centered cubic (fcc). In the body-centered modification, I, the center of the unit cell is symmetry-equivalent to the unit cell vertices (Figure 1.9). For the cubic symmetry system, the I-modification of the **Bravais** lattice is called body-centered cubic (bcc). Accounting of centered **Bravais** lattices increases their total amount up to 14.

In some cases, the choice of **Bravais** lattice is not unique. For example, fcc lattice can be represented as rhombohedral one with $a_R = a/\sqrt{2}$ and $\alpha = 60^\circ$ (Figure 1.10a). Rhombohedral lattice is a primitive one and comprises one atom per unit cell instead four atoms in the fcc unit cell. Similarly, bcc lattice can be represented in the rhombohedral setting with $a_R = a\sqrt{3}/2$ and $\alpha = 109.47^\circ$ (Figure 1.10b). In this case, the rhombohedral lattice comprises one atom per unit cell instead two atoms in the bcc

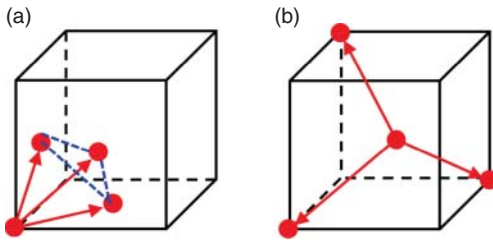


Figure 1.10 Lattice translations (red arrows) in the rhombohedral setting of the fcc (a) and bcc (b) lattices.

Table 1.1 Summary of possible symmetries in regular crystals.

Crystal symmetry	Bravais lattice type	Crystal classes (point groups)
Triclinic	P	$1, \bar{1}$
Monoclinic	P; B; or C	$m, 2, 2/m$
Orthorhombic	P; A, B, or C; I; F	$mm2, 222, mmm$
Tetragonal	P; I	$4, 422, \bar{4}, \bar{4}2m, 4/m, 4mm, 4/mmm$
Cubic	P; I (bcc); F (fcc)	$23, \bar{m}3, 432, \bar{4}3m, m\bar{3}m$
Rhombohedral (trigonal)	P (R)	$3, 32, 3m, \bar{3}, \bar{3}m$
Hexagonal	P	$6, 622, \bar{6}, \bar{6}2m, 6/m, 6mm, 6/mmm$

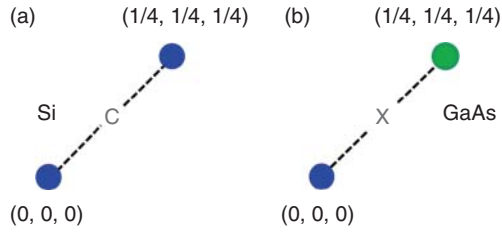
unit cell. We will widely use these settings in Chapter 2 considering the shapes of **Brillouin** zones. Minimizing number of atoms in the unit cell substantially reduces the calculation complexity of different physical properties in crystals.

Symmetry systems, types of **Bravais** lattices, and distribution of crystal classes (point groups) among them are summarized in Table 1.1.

The number of high-order symmetry elements, i.e. the threefold, fourfold, and sixfold rotation axes, which can simultaneously appear in a crystal, is also symmetry limited. For threefold rotation axis, this number may be one, in trigonal classes, or four, in cubic classes; for fourfold rotation axes – one in tetragonal classes or three in some cubic classes, while for sixfold rotation axis – only one in all hexagonal classes (see Appendix 1.A).

The presence or absence of an inversion center in a crystal is of utmost importance to many physical properties. For example, ferroelectricity and piezoelectricity (see Chapter 12) do not exist in centro-symmetric crystals, i.e. in those having inversion center. In this context, it is worth to note that any **Bravais** lattice is centro-symmetric. For primitive lattices, this conclusion follows straightforwardly from Eq. (1.1). Centered (non-primitive) **Bravais** lattices certainly do not refute this statement (Figures 1.8 and 1.9). However, only 11 crystal classes of total 32, in fact, are centro-symmetric. Even for high cubic symmetry, only two classes are centro-symmetric, i.e. $m\bar{3}$ and $m\bar{3}m$ (Table 1.1). Evidently, the loss of an inversion center can happen in crystals, which are built of several **Bravais** lattices, their origins being shifted relative to each other. We stress that it is necessary, but not

Figure 1.11 The presence of inversion center (**C**) in diamond structure (a) and its loss (**X**) in zinc-blende structure (b). Dissimilar atoms are indicated by different colors.



sufficient condition for the loss of inversion center. For illustration, let us consider Si (diamond structure) and GaAs (zinc blende or sphalerite structure) crystals. Both comprise two fcc lattices shifted relative to each other by one quarter of a space cube diagonal. The difference is that in silicon these sub-lattices are occupied by identical atoms (Si), whereas in GaAs – separately by Ga and As. In a result, Si is centro-symmetric (class $m\bar{3}m$) that can be easily proved by setting inversion center at point $(1/8, 1/8, 1/8)$, i.e. in the middle between the origins of two centro-symmetric fcc Si sub-lattices (Figure 1.11a). This recipe can hardly be used in case of GaAs since there is no symmetry operation that converts Ga to As (Figure 1.11b). Therefore, GaAs is non-centro-symmetric crystal belonging to class $4\bar{3}m$ and revealing significant piezoelectric effect.

Combining local symmetry elements with translations creates novel elements of spatial symmetry – glide planes and screw axes. Therefore, spatial symmetry is a combination of local (point) symmetry and translational symmetry. As a result, 32 point groups + 14 **Bravais** lattices produce 230 space groups describing all possible variants of crystal symmetry, associated with charge distributions, i.e. related to geometrical points and polar vectors. Magnetic symmetry, linked to magnetic moments (axial vectors, see Section 1.2), will be discussed in Chapter 11.

1.2 Symmetry and Physical Properties in Crystals

Crystal symmetry imposes tight restrictions on its physical properties. Term “properties” relates to those that can be probed by regular (macroscopic) optical, mechanical, electrical, and other measurements, averaging over the actual atomic-scale periodicity of physical characteristics. Note that complete spatial symmetry of the crystal is revealed in diffraction measurements using quantum beams (X-rays, neutrons, electrons) with wavelengths comparable with translational periodicity. Note that crystal characteristics, even averaged over many translation periods, show anisotropy which is dictated by the crystal point group. Within this averaged approach, the symmetry constraints are formulated by means of the so-called **Neumann’s** principle: the point group of the crystal is a sub-group of the group describing any of its physical properties. In simple words, the symmetry of physical property of the crystal cannot be lower than the symmetry of the crystal: it may be only equivalent or higher.

In practical terms, it means that if physical property is measured along certain direction within the crystal and then the atomic network is transformed according

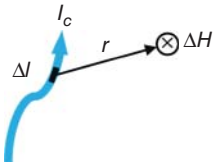


Figure 1.12 Illustration of the **Biot–Savart** law (Eq. (1.7)).

any symmetry element of its point group and measurement repeats, we expect to obtain the measurable effect of the same magnitude and sign as before. Any deviation will contradict particular crystalline symmetry and, thus, the **Neumann’s** principle. Using mathematical language, physical properties are, generally, described by tensors of different rank, for which the transformation rules under local symmetry operations are well-known. Tensor rank defines the number of independent tensor indices, i, k, l, m, \dots , each of them being run between 1 and 3, if the 3D space is considered. In most cases, physical property is the response to external field applied to the crystal. Note that external fields are also described by tensors, which are called field tensors to distinguish them from crystal (material) tensors.

Tensors of zero rank are scalars. It means that they do not change at all under coordinate transformations related to symmetry operations. As an example of scalar characteristics, we can mention the mass density of a crystal. Tensor of rank one is a vector. It has one index $i = 1, 2, 3$, which enumerates vector projections on three mutually perpendicular coordinate axes within **Cartesian (Descartes)** coordinate system. It is easy to point out field vectors, for example, an applied electric field, \mathcal{E}_i , or electric displacement field, D_i . As crystal vector, existing with no external fields, one can recall the vector of spontaneous polarization, P_i^s , in ferroelectric crystals (see Chapter 12). Spontaneous polarization, as well as polarization, P_i , induced by external electric field, is defined as the sum of elementary dipole moments per unit volume. Note that polarization \mathbf{P} is polar vector having three projections, P_i , as e.g. radius-vector \mathbf{r} (with projections, x_i). There exist also axial vectors (or pseudo-vectors), i.e. vector products (cross products) of polar vectors, which are used to describe magnetic fields and magnetic moments. In fact, magnetic field, $\Delta\mathbf{H}$, produced by the element $\Delta\mathbf{l}$ of a conducting wire carrying electric current, I_c , is described by the **Biot–Savart** law:

$$\Delta\mathbf{H} = \frac{I_c [\Delta\mathbf{l} \times \mathbf{r}]}{4\pi r^3} \quad (1.7)$$

where \mathbf{r} is the radius-vector connecting the element $\Delta\mathbf{l}$ and the observation point (see Figure 1.12). In turn, magnetic dipole moment, μ_d , is defined as an integral over the volume containing the current density distribution \mathbf{J} :

$$\mu_d = \frac{1}{2} \iiint_V [\mathbf{r} \times \mathbf{J}] dV \quad (1.8)$$

Axial vectors are considered when analyzing magnetic symmetry and magnetic symmetry groups (Chapter 11).

Tensor of rank 2 has two independent indices $i, k = 1, 2, 3$. As a rule, it linearly connects two vectors, e.g. the vectors of the electric displacement field, D_i , and external electric field, \mathcal{E}_k , i.e. $D_i = \sum_{k=1}^3 \varepsilon_{ik} \mathcal{E}_k$, as tensor of dielectric permittivity, ε_{ik} , does

(see Chapter 8). Another example is the density of electric current, J_i , and electric field, \mathcal{E}_k , connected by the electrical conductivity tensor ρ_{ik} , i.e. $J_i = \sum_{k=1}^3 \rho_{ik} \mathcal{E}_k$ (see Chapter 4). In further analyses, we will omit the summation symbols and use the reduced record (according to the **Einstein** convention) for tensor relationships, e.g.

$$D_i = \varepsilon_{ik} \mathcal{E}_k \quad (1.9)$$

$$J_i = \rho_{ik} \mathcal{E}_k \quad (1.10)$$

There are two important field tensors of second rank, which are in common use. These are the stress and strain tensors. Stress tensor, σ_{ik} , connects vector of external force, F_i , applied to a certain crystal area, ΔS , and unit vector, \hat{n}_k , normal to this area:

$$F_i = \sigma_{ik} \Delta S \hat{n}_k \quad (1.11)$$

Based on the mechanical equilibrium of the stressed solid, it is possible to prove that stress tensor (Eq. (1.11)) is symmetric one, i.e. $\sigma_{ik} = \sigma_{ki}$. Regarding strain tensor, it connects the deformation vector, u_i , in the vicinity of a given point and the radius-vector of this point, x_i . Deformation vector determines the difference in the distances between closely located points near x_i in the deformed and non-deformed states of the crystal. To provide local information on the deformed state, strain tensor, e_{ik} , is defined in the differential form:

$$e_{ik} = \frac{1}{2} \left(\frac{du_i}{dx_k} + \frac{du_k}{dx_i} \right) \quad (1.12)$$

Evidently, the strain tensor, defined by Eq. (1.12), is symmetric one, i.e. $e_{ik} = e_{ki}$.

Furthermore, inter-atomic distances within a crystal are also changed upon heating (see Chapter 3). In that sense, a crystal heated up to some temperature, T_1 , is in different “deformation” state as compared with its initial state at temperature, T_0 . Thus produced relative change in lattice parameters is mathematically equivalent to strain (Eq. (1.12)). Tensor of second rank, which relates e_{ik} to the temperature increase, $\Delta T = T_1 - T_0$ (tensor of rank zero, i.e. scalar), is called as tensor of linear expansion coefficients, α_{ik} :

$$e_{ik} = \alpha_{ik} \Delta T \quad (1.13)$$

Note that both crystal states, at $T = T_0$ and $T = T_1$, are thermodynamically equilibrium states at respective temperatures, and, therefore, no elastic energy is stored in such “deformed crystal,” whenever the temperature change is homogeneous across the crystal. The only energy difference between these two states is in free energy, which is temperature dependent.

Tensor of second rank may also connect a scalar and two vectors, as tensor of dielectric permittivity, ε_{ik} , does for energy density, W_e , of electromagnetic field within a crystal:

$$W_e = \frac{D_i \mathcal{E}_i}{2} = \frac{1}{2} \varepsilon_{ik} \mathcal{E}_i \mathcal{E}_k \quad (1.14)$$

By using tensor representation for the electric displacement field (see Eq. (1.9)), we find that the energy density is quadratic with respect to the applied electric field, \mathcal{E}_i .

Tensor of third rank has three indices $i, k, l = 1, 2, 3$. It connects tensor of second rank and vector, e.g. stress, σ_{ik} , and induced electric polarization, P_i :

$$P_i = d_{ikl}\sigma_{kl} \quad (1.15)$$

as for direct piezoelectric effect, or strain, e_{ik} , and applied electric field, \mathcal{E}_l :

$$e_{ik} = d_{lik}\mathcal{E}_l \quad (1.16)$$

for converse piezoelectric effect, both discussed in detail in Chapter 12. Another example is tensor, r_{lik} , of the linear electro-optic effect (the **Pockels** effect, also mentioned in Chapter 12). This tensor of third rank connects the change, Δn_{ik} , of refractive index, n , (which can be described in terms of the second rank tensor) under applied electric field, with the electric field vector, \mathcal{E}_l :

$$\Delta\left(\frac{1}{n^2}\right)_{ik} = r_{lik}\mathcal{E}_l \quad (1.17)$$

For the fourth rank tensor, there are several optional ways for its construction. It may connect two tensors of rank 2, e.g. stress, σ_{ik} , and strain, e_{lm} , as the stiffness tensor, C_{iklm} (tensor of elastic modules used in Chapter 3), does:

$$\sigma_{ik} = C_{iklm}e_{lm} \quad (1.18)$$

Similar tensor object, π_{iklm} , is used to describe the photo-elastic effect in crystals, which provides the change of refractive index under applied stress:

$$\Delta\left(\frac{1}{n^2}\right)_{ik} = \pi_{iklm}\sigma_{lm} \quad (1.19)$$

Another possibility is to connect tensor of second rank (e.g. strain tensor, e_{ik}) and two vectors (e.g. quadratic form of electric field, $\mathcal{E}_l \mathcal{E}_m$) as for electrostriction effect, g_{iklm} :

$$e_{ik} = g_{iklm}\mathcal{E}_l\mathcal{E}_m \quad (1.20)$$

or changes in refractive index, as a function of quadratic form of electric field, as for quadratic electro-optic effect, r_{iklm} (see Chapter 12):

$$\Delta\left(\frac{1}{n^2}\right)_{ik} = r_{iklm}\mathcal{E}_l\mathcal{E}_m \quad (1.21)$$

Eqs. (1.20, 1.21) describe the second order (quadratic) effects in the induced strain and change of refractive index, respectively, as a result of electric field application to a crystal. Tensor of rank 4 may also interconnect scalar quantity with two tensors of the second rank, as the stiffness tensor does when one calculates the density of elastic energy, W_{el} , stored within a crystal:

$$W_{el} = \frac{1}{2}\sigma_{ik}e_{ik} = \frac{1}{2}C_{iklm}e_{ik}e_{lm} \quad (1.22)$$

Therefore, using tensor representation of applied stress via induced strain (Eq. (1.18)), we find the density of elastic energy to be quadratic with respect to the induced strain. Tensors of rank higher than 4 describe high-order effects in the interaction between external fields and materials. These effects are regularly weak and, hence, are not discussed here.

Tensors of different ranks are appropriately transformed under local symmetry operations. All these operations can be exemplified as certain rotations of coordinate system, in which tensors are defined. Transformed tensor forms are compared with the initial ones, and, on this basis, symmetry restrictions on physical properties are imposed, to be in accordance with **Neumann's** principle. Based on this comparison, the zero tensor components can be determined, as well as symmetry-mediated relationships between non-zero tensor components. More information on symmetry aspects in crystals can be found in the dedicated crystallography books.

Additional interesting and important physical phenomenon, also related to symmetry operations, is twinning in crystals. For example, it stands behind the crystallography of ferroelectric domains (see Chapter 12) and is one of the channels of plastic deformation in crystals being competitive with dislocation glide. We stress that in terms of crystallography, twinning always is the result of symmetry operations, but those not belonging to the point group of a specific crystal. More information about twinning in crystals is given in Appendix 1.B.

1.3 Wave Propagation in Periodic Media and Construction of Reciprocal Lattice

With no doubts, leading crystal symmetry is translational symmetry, which is of great importance to the foundations of solid state physics. In particular, it allows us to deeply understand the essential features of wave propagation in periodic media, which influence a majority of physical phenomena in crystals. We start now with the symmetry-based analysis of wave propagation following the ideas of **Leon Brillouin**.

Let us consider, first, the propagation of the plane electron wave, $Y = Y_0 \exp[i(\mathbf{k}\mathbf{r} - \omega t)]$, in a homogeneous medium. Here, Y_0 is the wave amplitude, \mathbf{k} is the wavevector, and ω is the wave angular frequency, whereas \mathbf{r} and t are the spatial and temporal coordinates. The phase of plane wave is $\varphi = (\mathbf{k}\mathbf{r} - \omega t)$, i.e. $Y = Y_0 \exp(i\varphi)$. According to the **Emmy Noether** theorem, the homogeneity of space leads to the momentum conservation law. It means that an electron wave having wavevector, \mathbf{k}_i , at a certain point in its trajectory, will continue to propagate with the same wavevector since the wavevector, \mathbf{k} , is linearly related to the momentum, \mathbf{P} , via the reduced **Planck** constant \hbar , i.e. $\mathbf{P} = \hbar\mathbf{k}$. The latter relationship follows from the de **Broglie** definition of the particle wavelength (**de Broglie** wavelength) via its momentum: $\lambda = \frac{2\pi}{k} = \frac{h}{P}$.

The situation drastically changes for a non-homogeneous medium, in which the momentum conservation law, generally, is not valid because of the breaking of the aforementioned symmetry (homogeneity of space). Consequently, in such a medium, one can find wavevectors, \mathbf{k}_f , differing from the initial wavevector, \mathbf{k}_i .

Our focus here is on a non-homogeneous medium with translational symmetry, which comprises scattering centers in specific points, \mathbf{r}_s , given by Eq. (1.1). Based on the translational symmetry only, we can say that in an infinite medium with no absorption, the magnitude of plane wave, Y , should be the same near each lattice node. It means that the amplitude, Y_0 , is the same at all points, \mathbf{r}_s , whereas the phase,

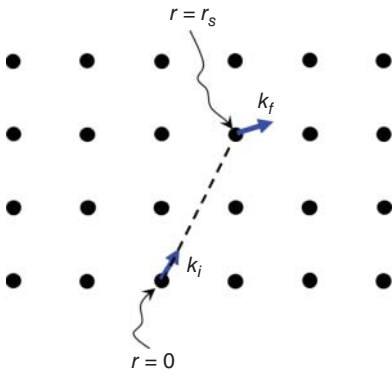


Figure 1.13 Illustration of the wave scattering in a periodic medium.

$\varphi = \mathbf{k}\mathbf{r} - \omega t$, can differ by an integer number m of 2π . Let us suppose that the plane wave has wavevector, \mathbf{k}_i , at starting point $\mathbf{r}_0 = 0$ and time moment, $t_0 = 0$, and hence $\varphi(0) = 0$. If so, at point \mathbf{r}_s , the phase, $\varphi(\mathbf{r}_s)$, should be equal:

$$\varphi(\mathbf{r}_s) = \mathbf{k}_f \mathbf{r}_s - \omega t = 2\pi m \quad (1.23)$$

Note that the change of the wavevector from \mathbf{k}_i to \mathbf{k}_f physically means that the wave experiences scattering in point, \mathbf{r}_s (Figure 1.13). For elastic scattering (with no energy change):

$$|\mathbf{k}_f| = |\mathbf{k}_i| = |\mathbf{k}| = \frac{2\pi}{\lambda} \quad (1.24)$$

where λ is the electron wavelength. Furthermore, the time interval, t , for wave propagation between points, $\mathbf{r}_0 = 0$ and \mathbf{r}_s , equals

$$t = \frac{\mathbf{k}_i \mathbf{r}_s}{|\mathbf{k}_i| V_p} \quad (1.25)$$

where

$$V_p = \frac{\omega}{|\mathbf{k}|} \quad (1.26)$$

is the phase wave velocity. Substituting Eqs. (1.24–1.26) into Eq. (1.23) yields:

$$\varphi(\mathbf{r}_s) = (\mathbf{k}_f - \mathbf{k}_i) \mathbf{r}_s = 2\pi m \quad (1.27)$$

Introducing a new vector, \mathbf{G} , which is called vector of reciprocal lattice,

$$2\pi \mathbf{G} = \mathbf{k}_f - \mathbf{k}_i \quad (1.28)$$

and combining Eqs. (1.27, 1.28), we find

$$\mathbf{G} \cdot \mathbf{r}_s = m \quad (1.29)$$

According to Eqs. (1.28, 1.29), different values of $\mathbf{k}_f = \mathbf{k}_i + 2\pi \mathbf{G}$ are permitted in a periodic medium, but only those that provide scalar products of certain vectors, \mathbf{G} , with all possible vectors, \mathbf{r}_s , to be integer numbers, m . By substituting Eq. (1.1) into Eq. (1.29), we finally obtain:

$$\mathbf{G} \cdot (n_1 \mathbf{a}_1 + n_2 \mathbf{a}_2 + n_3 \mathbf{a}_3) = m \quad (1.30)$$